JOURNAL OF BACTERIOLOGY, Feb. 1997, p. 1211–1218 Vol. 179, No. 4
0021-9193/97/$04.00+0

The Lipoprotein VirB7 Interacts with VirB9 in the Membranes of *Agrobacterium tumefaciens*

CHRISTIAN BARON,† YVONNE R. THORSTENSON,‡ AND PATRICIA C. ZAMBRYSKI*

Department of Plant and Microbial Biology, University of California at Berkeley, Berkeley, California 94720

Received 6 September 1996/Accepted 9 December 1996

VirB9 and VirB7 are essential components of the putative VirB membrane channel required for transfer of the T-complex from *Agrobacterium tumefaciens* into plants. In this report, we present a biochemical analysis of their interaction and cellular localization. A comparison of relative electrophoretic mobilities under nonreducing and reducing conditions suggested that they form thiol-sensitive complexes with other proteins. Two-dimensional gel electrophoresis identified one complex as a heterodimer of VirB9 and VirB7 covalently linked by a disulfide bond, as well as VirB7 homodimers and monomers. Immunoprecipitation with VirB9-specific antiserum isolated the heterodimeric VirB9-VirB7 complex. Incubation with reducing agent split the complex into its constituent VirB9 and VirB7, which further confirmed linkage via cysteine residues. The interaction between VirB9 and VirB7 also was observed in the yeast two-hybrid system. Membrane attachment of VirB9-VirB7 may be conferred by lipoprotein modification, since labeling with [^{3}H]palmitic acid in *A. tumefaciens* verified that VirB7 is a lipoprotein associated with VirB9. VirB9 and VirB7 showed equal distribution between inner and outer membranes, in accord with their proposed association with the transmembrane VirB complex.

Agrobacterium tumefaciens infects plants at wound sites and transfers a portion of its genetic material to the nucleus of its host. After integration into chromosomal DNA, expression of the encoded genes redirects plant metabolism toward production of gall-promoting phytohormones and of conjugates of amino acids and sugars (opines), used by *Agrobacterium* as carbon and nitrogen sources. Several chromosomally encoded products as well as specific virulence (*vir*) products encoded on the Ti (tumor-inducing) plasmid are required for this genetic colonization of plants (21, 55, 59). The transferred genetic material is a single-stranded copy of a specific region of the Ti plasmid, called the T-strand. Two *vir* products, VirD1 and VirD2, are essential for excision of the T-strand from the Ti plasmid (23, 35, 43). The T-strand is transferred to the plant cell presumably as a complex with Vir proteins, the T-complex (7, 10, 11, 34, 48, 57, 58).

Transfer of the T-complex from *A. tumefaciens* to plant cells requires 10 VirB proteins and VirD4. VirB1, the 11th component of the *virB* operon, is not absolutely required for genetic transformation of plants, but its deletion reduces efficiency 100-fold (6). These proteins are proposed to form a transmembrane channel that spans the bacterial inner and outer membranes and may transfer the T-complex into the plant cytoplasm. Different lines of evidence support this model. First, sequence analysis predicted membrane or periplasmic localization of most *virB*-encoded proteins (27, 46, 51, 52). Second, PhoA fusions and susceptibility to proteases confirmed the periplasmic location of hydrophilic VirB proteins with signal peptides (VirB1, VirB5, VirB7, and VirB9) and demonstrated periplasmic domains of membrane-associated proteins (VirB2, VirB3, VirB6, VirB8, and VirB10) (4, 14). Third, cell fractionation and immunoelectron microscopy localized most VirB proteins and VirD4 in the membranes (3a, 5, 9, 14, 16, 17, 25, 33, 44, 45, 49–51). Many proteins are distributed equally between inner and outer membranes, in accord with a transmembrane structure held together by protein-protein interactions. Fourth, homologies of VirB proteins and VirD4 to components of bacterial conjugation and protein secretion systems suggest a common mechanism for traffic of DNA-protein complexes and protein toxins (26, 30, 53). Interestingly, the putative VirB channel may transfer VirE2 (7, 34) and VirF (38) into plant cells. Although this transfer has yet to be shown directly, the diversity of potentially transported proteins is reminiscent of other bacterial secretion systems with multiple recognized substrates (39, 40).

Studies on protein-protein interactions and assembly of the putative VirB channel have been performed to address the mechanism of T-complex transfer. Analysis of in-frame deletions in all *virB* genes showed that loss of some VirB proteins, such as VirB7 and VirB9, drastically reduced steady-state levels of several others, such as VirB4, VirB5, VirB8, VirB10, and VirB11 (6). Also, VirB4 was required for stability and membrane targeting of VirB3 (25). Complementation of *virB7* and *virB9* deletion mutants restored steady-state levels of other VirB proteins, further demonstrating their stabilizing effect on the putative channel (15). These results suggested protein-protein interactions between components of the VirB channel localized to the outer membrane (VirB7 and VirB9), the periplasm and inner membrane (VirB5, VirB8, and VirB10), and the cytoplasm (VirB4 and VirB11).

Since VirB9 and VirB7 apparently stabilize the VirB membrane complex, their interaction was further characterized. Biochemical and genetic studies showed that VirB9 and VirB7 form a cysteine-linked complex in the *Agrobacterium* periplasm and identified the cysteine residues involved (1, 14, 15, 47). Here, we extend the analysis of the VirB9-VirB7 interaction by analysis of complex formation at different time points after *vir* gene induction, using two-dimensional gel electrophoretic techniques and the two-hybrid system in *Saccharomyces cerevi-*

* Corresponding author. Mailing address: University of California at Berkeley, Department of Plant and Microbial Biology, 111 Koshland Hall, Berkeley, CA 94720. Phone: (510) 643-9203. Fax: (510) 642-4995. E-mail: zambrysk@mendel.berkeley.edu.

† Present address: Lehrstuhl für Mikrobiologie der Universität München, D-80638 Munich, Germany.

‡ Present address: Stanford DNA Sequencing and Technology Center, Palo Alto, CA 94304.

TABLE 1. Strains and plasmids used

Strain or plasmid	Relevant characteristics	Reference or source
Strains		
A. tumefaciens GV3850	Crb^r; tumorigenic T-DNA replaced with pBR322 *amp* gene	56
E. coli JM109	*endA1 gyrA96 thi hsdR17 supE44 recA1 relA1* Δ(*lac-proAB*) (F′ *traD36 proAB*$^+$ *lacI*^{q} *lacZ*ΔM15)	54
S. cerevisiae Y153	*MAT***a** *leu2-3,112 ura3-52 trp1-901 his3-*Δ*200 ade2-101 gal4*Δ *gal80*Δ *URA3::GAL-lacZ LYS2::GAL-HIS3*	12
Plasmids		
pGK217	Crb^r; pUC119 containing *virB* operon and truncated *virG*	27
pET3b::E2	Crb^r; overexpresses VirE2 of *Agrobacterium* in fusion with 12 amino acids of pET3b	11
pH$_6$TRXFUS-D2	Crb^r; in-frame fusion of *virD2* to histidine-tagged *trx* gene of pTRXFUS (29)	3a
pH$_6$TRXFUS-B7	Crb^r; in-frame fusion of *virB7* to histidine-tagged *trx* gene of pTRXFUS (29)	3a
pAS2	Crb^r; for construction of fusions to DBD of GAL4	12
pACTII	Crb^r; for construction of fusions to AD of GAL4	S. Elledge
pAS2-VirB9	Crb^r; pAS2 with 0.9-kb *Nde*I/*Bam*HI *virB9* PCR fragment	This work
pAS2-VirE2	Crb^r; pAS2 with blunt-ended 1.7-kb *Bam*HI/*Sal*I *virE2* fragment from pET3b::E2 introduced into blunt-ended *Bam*HI site	This work
pACTII-VirB7	Crb^r; pACTII with 0.1-kb *Sma*I/*Xba*I *virB7* fragment	This work
pACTII-VirE2	Crb^r; pACTII with blunt-ended 1.7-kb *Bam*HI/*Sal*I *virE2* fragment from pET3b::E2 introduced into blunt-ended *Bam*HI site	This work
pACTII-VirD2	Crb^r; pACTII with blunt-ended 1.3-kb *Asp*718/*Bam*HI *virD2* fragment from pH$_6$TRXFUS-D2 introduced into blunt-ended *Bam*HI site	This work

siae. Earlier studies using *Escherichia coli* suggested that VirB7 is a lipoprotein (14). Here, we directly demonstrate that in *A. tumefaciens*, VirB7 is a lipoprotein that undergoes complex formation with VirB9. This report and the accompanying report showing that a processing product of VirB1 (VirB1*) interacts with the VirB complex via VirB9-VirB7 (3) strongly support transmembrane topology of the T-complex transfer apparatus that links the cytoplasm to the bacterial cell surface.

MATERIALS AND METHODS

Strains and growth conditions. *A. tumefaciens* GV3850 was grown as described previously (3). *E. coli* JM109 was grown in Luria broth containing appropriate antibiotics (carbenicillin at 100 μg/ml) for plasmid maintenance. *S. cerevisiae* Y153 was cultured in rich YEPD medium or, to select for maintenance of plasmids, in minimal medium as described previously (12). The strains and plasmids used are described in Table 1.

Protein analysis, cell fractionation, and immunological methods. Sodium dodecyl sulfate (SDS)-polyacrylamide gel electrophoresis (PAGE) in one and two dimensions (nonreducing in the first and reducing in the second) was performed in 12.5% polyacrylamide-containing gels, using a Tricine-SDS buffer system (42) to resolve low-molecular-mass proteins like VirB7 (4.5kDa). To resolve proteins larger than 20 kDa, 10% polyacrylamide gels and the Laemmli buffer system (28) were used. Western blotting, immunological detection of antigens, cell lysis, coimmunoprecipitation, and cell fractionation were performed as described previously (3). To avoid artifacts due to oxidation of free (reduced) sulfide groups, cells were incubated after harvest in 10 mM iodoacetamide for 10 min on ice.

Generation of VirB9-specific antiserum was described previously (49); antibodies against VirB7 were generated by immunization with a peptide conjugate prepared as follows. First, 3 mg of rabbit serum albumin (RSA; Sigma) was incubated with 0.8 mg of the heterobifunctional cross-linking agent SMPB (Pierce), dissolved in 25 μl of 1-methyl-2-pyrrolidinone, in a total volume of 100 μl of 0.2 M sodium phosphate buffer (pH 7.2) for 30 min at 23°C. Under these conditions, SMPB links to accessible lysines on RSA. Change of buffer pH and separation from nonreacted cross-linking agent was attained by chromatography of the modified carrier RSA over a 3-ml Sephadex G-25 column in 0.1 M sodium phosphate buffer (pH 6.5). Under these conditions, SMPB reacts with accessible cysteine residues. Thus, we coupled modified RSA with 2 mg of the 20-mer peptide (CKGPIFPLNVGRWQPTPSDL; amino acids 24 to 43 of VirB7) for 3 h at 23°C followed by extensive dialysis. The RSA-peptide conjugate was used for immunization of New Zealand White rabbits as described previously (49).

Crude VirB7-specific antiserum showed strong background reactions. Therefore, antibodies were affinity purified by binding and elution from polyvinylidene difluoride membrane strips (19) containing bound purified thioredoxin-VirB7 fusion protein (3a).

Labeling with [^{3}H]palmitic acid and autoradiography. Fifty-milliliter cultures of strain GV3850 were grown and *vir* induced with acetosyringone (AS) as described previously (3). At the time of induction, 1 mCi of [9,10-^{3}H(N)]palmitic acid (specific activity, 30 to 60 Ci/mmol; New England Nuclear) was added to induced and control cultures, which were then incubated for 18 h at 28°C. Cells were harvested, incubated for 10 min on ice in 10 mM iodoacetamide to block free sulfide groups, and lysed by boiling in Laemmli sample buffer without β-mercaptoethanol. Cell extracts were resolved by SDS-PAGE. For analysis in the second dimension, bands were excised, incubated in Laemmli sample buffer with 100 mM dithiothreitol (DTT) for 30 min, and applied to a second gel followed by SDS-PAGE. Prior to autoradiography, gels were incubated for 15 min in Amplify (Amersham), dried, and exposed to X-Omat AR film (Kodak).

Construction of recombinant plasmids. To test protein-protein interactions in the two-hybrid system in yeast, *vir* genes were fused in frame to the gene encoding the GAL4 DNA binding domain (DBD) of pAS2. For VirB9, its coding sequence from amino acid 22 on was amplified from 1 ng of pGK217 template (27) by PCR with the 22-mer oligonucleotide B9-5 (5′-GGCATATGGAAGAC ACGCCAAC-3′) and the 23-mer B9-3 (5′-GGGGATCCTGCTGATTGTCGT CG-3′), which introduced an *Nde*I site overlapping amino acid 22 of the coding sequence and a *Bam*HI site adjacent to the stop codon. Purified PCR product was digested with *Nde*I and *Bam*HI and ligated with similarly cut and shrimp alkaline phosphatase (SAP; United States Biochemicals)-treated plasmid pAS2, resulting in pAS2-B9. For VirE2, pET3b::E2 (11) was digested with *Bam*HI and *Sal*I. The resulting 1.7-kb fragment was purified, and single-stranded protruding ends were filled in with Klenow DNA polymerase (New England Biolabs), ligated with pAS2 cleaved with *Bam*HI and treated with Klenow DNA polymerase and SAP, resulting in pAS2-E2.

The GAL4 activation domain (AD) gene of pACTII was fused in frame to *vir* genes as follows. For VirB7, its coding sequence from amino acid 15 to the end was PCR amplified from 1 ng of pGK217 template with 30-mer oligonucleotide VirB7-5 (5′-GGTACCCGGGTGCCAGACAAACGATAAATT-3′) and 27-mer VirB7-3 (5′-AGAGTCTAGATCAGACCCCTTCATGGC-3′). Purified PCR product was restricted with *Sma*I and *Xba*I and then ligated with *Sma*I/*Xba*I-restricted pACTII, resulting in pACTII-B7. For VirD2, pH$_6$TRXFUS-D2 (3a) was restricted with *Asp*718 and *Bam*HI, and single-stranded protruding ends were filled in with Klenow DNA polymerase, ligated with pACTII restricted with *Bam*HI and treated with Klenow DNA polymerase and SAP, resulting in pACTII-D2. For VirE2, a 1.7-kb *Bam*HI/*Sal*I-restricted fragment from pET3b::E2 was purified, and single-stranded protruding ends were filled in with Klenow DNA polymerase, ligated with pACTII cleaved with *Bam*HI and treated with Klenow DNA polymerase and SAP, resulting in pACT-E2.

All PCR-derived constructs and the fusion points of subclones were verified by DNA sequencing by standard methods (41).

Test of protein-protein interactions in the two-hybrid system in yeast. Growth of *S. cerevisiae* Y153, transformation of recombinant plasmids, and determination of β-galactosidase activity were performed as described by Durfee et al. (12).

Image processing. The images presented in this report were generated after scanning of blots in a scanner (Microtek) at a resolution of 300 dots per inch and processed on a Power Macintosh 7100 computer with the software Photoshop 3.0. Prints were generated with a Phaser 440 printer (Tektronix).

RESULTS

Comparison of reducing and nonreducing electrophoresis reveals multiple forms of VirB7 and VirB9. When cell lysates were prepared by boiling in Laemmli sample buffer and re-

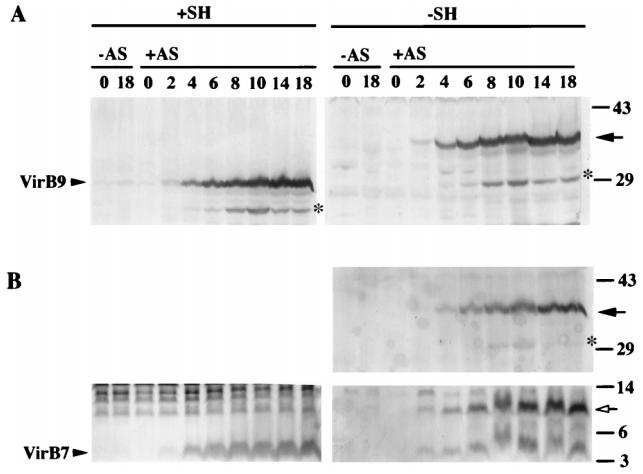

FIG. 1. Time course of synthesis of VirB7 and VirB9 measured on reducing and nonreducing gels. Samples from *vir*-induced GV3850 cultures (+AS) or uninduced control cultures (−AS) were taken every 2 h up to 18 h after *vir* induction. Cell lysates were subjected to SDS-PAGE under nonreducing (−SH) or reducing (+SH) conditions, transferred to polyvinylidene difluoride membranes, and subjected to analysis with VirB9 (A)- and VirB7 (B)-specific antibodies. The migration positions of VirB9 (31 kDa) and VirB7 (4.5 kDa) in reducing gels are indicated. VirB9- and VirB7-cross-reactive complexes visualized in nonreducing gels are indicated by black (36 kDa) and white (10 kDa) arrows, respectively. Putative degradation products of VirB9 (25 kDa under reducing conditions; 30 kDa under nonreducing conditions) are indicated by asterisks.

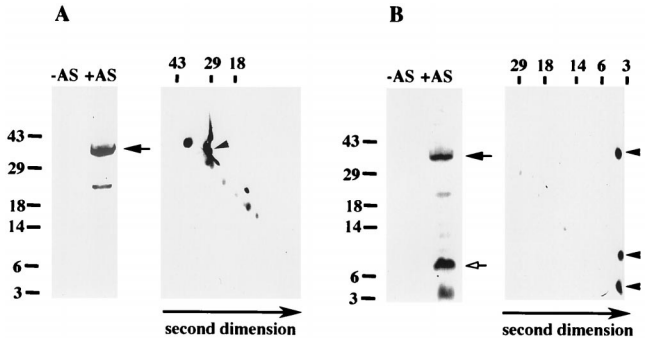

FIG. 2. Analysis of VirB9 and VirB7 complexes by two-dimensional SDS-PAGE. Cell extracts from *vir*-induced cultures (+AS) or uninduced control cultures (−AS) were lysed under nonreducing conditions and resolved by SDS-PAGE in the first dimension. Gel lanes containing proteins from induced extracts were excised after first-dimension SDS-PAGE, incubated in Laemmli sample buffer with 100 mM DTT to break disulfide bonds, and subjected to SDS-PAGE in the second dimension followed by Western blotting and detection with VirB9-specific (A) or VirB7-specific (B) antiserum. VirB9- and VirB7-cross-reactive complexes visualized in nonreducing first-dimension gels are indicated by black (36 kDa) and white (9 kDa) arrows, respectively. VirB9 (31 kDa) and VirB7 (4.5 kDa) detected after second-dimension SDS-PAGE are indicated by arrowheads.

solved by SDS-PAGE, 31-kDa VirB9 and 4.5-kDa VirB7 proteins were detected by Western blotting between 2 and 4 h after *vir* gene induction with AS, and maximum accumulation was reached after 10 h (Fig. 1). These molecular masses agree with the calculated molecular mass of VirB7 and with earlier results from our and other labs (1, 14, 49). In addition, a minor VirB9-cross-reacting species of 25 kDa was detected starting from 6 h after AS induction, which could be a degradation product (15).

However, Fig. 1 shows that preparation of lysates under nonreducing conditions resulted in a shift of the VirB9-cross-reacting species to 36 kDa; the species at 30 kDa could result from a similar approximately 5-kDa shift of the minor 25-kDa product. Omission of reducing agents also had dramatic consequences on the migration of VirB7-cross-reacting species. In addition to the 4.5-kDa protein, cross-reacting products at 9 and 36 kDa were detected. Interestingly, the ratio between the three species did not change significantly over the time course of induction, suggesting that the biochemical process involved causes rapid association of VirB7 and VirB9. The altered migration of VirB9 and VirB7 in nonreducing SDS-PAGE may be due to disulfide bond formation with other proteins. Inspection of the sequence of the mature proteins revealed that both contain one cysteine residue, at positions 24 of VirB7 and 262 of VirB9. The comigration of VirB9- and VirB7-cross-reacting species at 36 kDa after nonreducing SDS-PAGE suggested that these two proteins may form a heterodimeric complex via cysteine residues. Further, the relative migration of the 9-kDa VirB7-cross-reacting species suggested it may be a dimer of VirB7.

VirB9 forms a complex with VirB7. To analyze the composition of the putative heterodimeric 36-kDa (VirB9-VirB7) and homodimeric 9-kDa (VirB7-VirB7) complexes, cell lysates were analyzed by two-dimensional SDS-PAGE (nonreducing in the first dimension and reducing in the second dimension) and Western blotting. Analysis of the second-dimension separation with VirB9-specific antiserum shows that incubation with DTT released a protein of 31 kDa, the molecular mass of VirB9, from the 36-kDa complex detected in the first dimension (Fig. 2A). Analysis with VirB7-specific antiserum detected a protein of 4.5 kDa, the molecular mass of monomeric VirB7, released by DTT from the complexes of 36 and 9 kDa (Fig. 2B).

To further substantiate the composition of thiol-labile complexes, cells were lysed under nonreducing conditions by boiling in 2% SDS-containing buffer, a treatment that disrupts protein-protein interactions and protein-membrane associations but leaves covalent bonds intact (19). To allow antigen-antibody interaction, the lysate was diluted to 0.2% SDS followed by immunoprecipitation with VirB9-specific antiserum and protein A-Sepharose beads. Figures 3A and B show analysis of immunoprecipitates after SDS-PAGE and Western blotting with VirB9- and VirB7-specific antisera, respectively. Under nonreducing conditions, a 36-kDa complex cross-react-

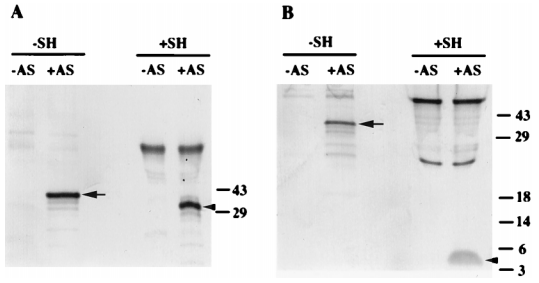

FIG. 3. Coimmunoprecipitation of VirB7 and VirB9. Cells from *vir*-induced cultures (+AS) or controls (−AS) were lysed and then subjected to immunoprecipitation with VirB9-specific antiserum and Protein A-Sepharose beads. Samples were boiled in sample buffer with (+SH) or without (−SH) β-mercaptoethanol, resolved by SDS-PAGE followed by Western blotting, and detected with VirB9-specific (A)- or VirB7-specific (B) antiserum. The VirB9- and VirB7-cross-reactive complex of 36 kDa visualized after nonreducing SDS-PAGE is indicated by arrows. VirB9 (31 kDa) and VirB7 (4.5 kDa) detected after reducing SDS-PAGE are indicated by arrowheads. The bands of higher molecular weight detected in lanes containing extracts from *vir*-induced cultures and controls probably correspond to light and heavy chains of antibodies used for immunoprecipitation.

TABLE 2. Interaction of Vir proteins detected with the two-hybrid system in yeast

Protein fusion to:		β-Galactosidase (U)[a]
DBD	AD	
VirB9	—[b]	<1
VirB9	VirB7	45
VirB9	VirE2	<1
VirB9	VirD2	<1
VirE2	—	<1
VirE2	VirB7	<1
VirE2	VirE2	48
VirE2	VirD2	<1

[a] Measured in *S. cerevisiae* Y153 as described in reference 12; mean of two to four independent experiments.
[b] —, pACTII alone.

ing with VirB9 and VirB7 antibodies was detected in immunoprecipitates from *vir*-induced cells. Incubation of the samples with β-mercaptoethanol dissociated the covalent thiol bond and released VirB9 (31 kDa) and VirB7 (4.5 kDa).

Thus, the 36-kDa complex contains VirB7 and VirB9 linked by a disulfide bond. The 9-kDa complex contains VirB7 linked by a disulfide bond to another small protein, most likely VirB7. Another potential partner of VirB7 in the 9-kDa complex could be the processed form of VirB2 (5 kDa), but Western blotting analysis showed that VirB2 does not form complexes of 9 kDa or higher molecular mass under nonreducing conditions (data not shown). However, we cannot exclude that VirB7 binds to an unidentified small *Agrobacterium* protein.

The above-mentioned results confirm published data from other labs (1, 14, 15). Analysis of the time course of induction shows that monomeric VirB9 cannot be detected in lysates prepared under nonreducing conditions, suggesting that complex formation with VirB7 is fast and/or free VirB9 is unstable (6, 15). In contrast to published work (47), we reproducibly detect significant amounts of monomeric VirB7 in lysates prepared under nonreducing conditions.

Interaction of Vir proteins assayed by the two-hybrid system in yeast. To gain independent evidence for specific interaction between VirB7 and VirB9, we used the two-hybrid system in yeast. In-frame fusions of several Vir proteins to the DBD or the AD of the GAL4 transcriptional activator were generated, and pairwise combinations of these plasmids were transformed into *S. cerevisiae* Y153, which carries a chromosomal fusion of the *GAL1* promoter to the *lacZ* gene. Interaction of proteins fused to the DBD and AD of GAL4 leads to activation of transcription and can be measured as β-galactosidase activity. To assess the suitability of the two-hybrid system for the study of protein-protein interactions in *Agrobacterium*, we first tested an interaction that had previously been suggested by biochemical experiments. VirE2 is a cooperative single-stranded DNA (ssDNA) binding protein that may be part of the T-complex (10, 11, 57, 58). When VirE2 fusions to DBD and AD were coexpressed in strain Y153, we observed transcriptional activation, in accord with its cooperative binding to ssDNA (Table 2). Control experiments showed that VirE2-DBD and VirE2-AD (not shown) fusion proteins do not activate transcription by themselves and do not bind in a nonspecific manner to other proteins such as VirB7 or VirD2 fusions. Next, we cotransformed Y153 with plasmids expressing fusions of VirB9 to the DBD and VirB7 to the AD and found strong transcriptional activation. Control combinations of the VirB9-DBD or VirB9-AD (not shown) plasmid with plasmids expressing fusions of VirE2 and VirD2 gave no detectable transcriptional activation, showing specificity of the VirB9-VirB7 interaction. However, the reciprocal experiment could not be performed, because DBD-VirB7 fusion proteins activated transcription on their own. Thus, we were not able to assess the putative VirB7-VirB7 interaction with this method (data not shown).

Labeling with [^{3}H]palmitic acid confirms that VirB7 is a lipoprotein that undergoes complex formation with VirB9. Sequence analysis found a signal peptidase II (SPII) processing site in VirB7. By analogy to the lipoprotein processing pathway in *E. coli* (20), VirB7 may undergo modifications. For example, cysteine residue 15 may be modified by addition of glycerol via a thioether linkage, followed by esterification of the glycerol with fatty acids, cleavage after amino acid 14 by SPII, and attachment of a fatty acid to the amino group of the N-terminal cysteine. Incorporation of radioactive fatty acids provides a means to assay lipoprotein labeling of VirB7, and Fernandez et al. (14) showed incorporation of radioactive [^{3}H]palmitic acid into VirB7 and VirB7::PhoA fusion proteins in *E. coli*. Also, globomycin inhibited lipoprotein processing in *Agrobacterium*, and small amounts of a putative precursor protein were detected by Western blotting (14).

However, we wanted to study lipoprotein processing of VirB7 and its complex formation with VirB9 in *Agrobacterium*; therefore, we incubated strain GV3850 with or without AS in the presence of [^{3}H]palmitic acid. After *vir* induction for 18 h, cells were harvested and lysed by boiling in Laemmli sample buffer without β-mercaptoethanol and resolved by SDS-PAGE (Fig. 4A). Extracts from induced and noninduced cells showed high background labeling of low-molecular-weight products, so that labeled AS-induced 9-kDa (VirB7 homodimer) or 4.5-kDa (VirB7 monomer) products were not detectable. We and others (14) attribute this background to incorporation of palmitic acid into other small lipoproteins or lipopolysaccharides. However, only *vir*-induced cells synthesized a 36-kDa labeled product with the molecular mass of the VirB9-VirB7

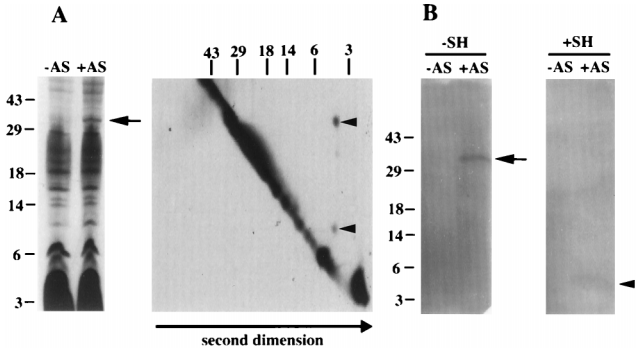

FIG. 4. Labeling of VirB7 with [^{3}H]palmitic acid and coimmunoprecipitation of ^{3}H-labeled VirB7-VirB9. (A) *A. tumefaciens* cultures were grown in the presence of [^{3}H]palmitic acid and either *vir* induced (+AS) or not induced (controls; −AS). Lysates were prepared under nonreducing conditions and resolved by SDS-PAGE in the first dimension. A lane containing extract from induced cells was excised, incubated in Laemmli sample buffer with 100 mM DTT to break disulfide bonds, and subjected to SDS-PAGE in the second dimension followed by treatment of the gel with Amplify, drying, and autoradiography. (B) Coimmunoprecipitation of radiolabeled VirB7 and VirB9. Cells from *vir*-induced cultures (+AS) or controls (−AS) grown with [^{3}H]palmitic acid were lysed and then subjected to immunoprecipitation with VirB9-specific antiserum and protein A-Sepharose beads. Samples were boiled in sample buffer with (+SH) or without (−SH) β-mercaptoethanol, and resolved by SDS-PAGE; this was followed by treatment of the gel with Amplify, drying, and autoradiography. The radiolabeled 36-kDa complex of VirB7 and VirB9 is indicated by arrows. VirB7 (4.5 kDa) detected after treatment with reducing agents is indicated by arrowheads. This band was detected only after extended exposure (3 months) and is clearly visible on the original film.

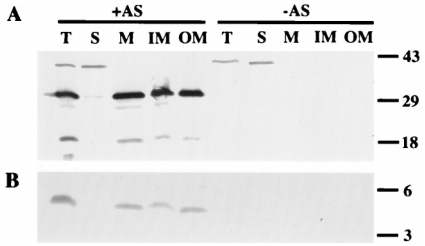

FIG. 5. Cellular localization of VirB7 and VirB9. Shown is analysis of Western blots with VirB9-specific (A) and VirB7-specific (B) antibodies after SDS-PAGE. Cells from *vir*-induced cultures (+AS) and control cultures (−AS) were lysed, and cell compartments were separated by differential centrifugation. Lanes: T, total cell lysates; S, soluble fraction; M, total membrane fraction; IM, inner membrane; OM, outer membrane. Separation of inner and outer membranes by isopycnic sucrose gradient centrifugation was monitored by marker enzyme NADH oxidase (for inner membrane) and content of 2-keto-3-deoxyoctonate (for outer membrane) as described in reference 3.

heterodimer (see above). To confirm the presence of radiolabeled VirB7 in the complex, the entire gel lane containing proteins from *vir*-induced cells was excised after first-dimension SDS-PAGE, incubated with DTT to break disulfide bonds, and then subjected to second-dimension SDS-PAGE. Figure 4A shows that incubation with DTT released radiolabeled products of 4.5 kDa, presumably monomeric VirB7, from complexes migrating at 36 and 9 kDa in the first dimension. This finding parallels the results of our Western blotting analysis of VirB9-VirB7 heterodimers and VirB7-VirB7 homodimers (Fig. 2). Control experiments with extracts from noninduced cells showed no labeled 4.5-kDa products after second-dimension SDS-PAGE (data not shown). The radiolabeled 36-kDa complex was also isolated by immunoprecipitation with VirB9-specific antiserum, and VirB7 could be released by incubation with DTT (Fig. 4B). Taken together, these experiments confirmed that VirB7 is a lipoprotein in *Agrobacterium*, and the fatty acid modification may link the otherwise hydrophilic protein to the membranes. Also, immunoprecipitation with VirB9-specific antiserum suggested that complex formation with VirB9 occurs after modification of VirB7.

Cellular localization of VirB7 and VirB9. The amino acid residue adjacent to the N-terminal cysteine of processed lipoproteins (+2) determines their localization in *E. coli*. Lipoproteins carrying amino acids other than aspartate at this position localize in the outer membrane (18, 37), and since VirB7 carries an asparagine residue there, its targeting to the outer membrane was predicted. Sequence analysis of VirB9 predicts export of the hydrophilic protein into the periplasm, but it may localize to the outer membrane due to its covalent attachment to VirB7. To test their localization, *vir*-induced and uninduced agrobacteria were lysed by passage through a French pressure cell, total membranes were separated from the soluble fraction (periplasm and cytoplasm) by ultracentrifugation, and inner and outer membranes were further separated by isopycnic sucrose gradient fractionation. Figure 5 shows that both VirB7 and VirB9 localized almost exclusively in the membrane fraction of induced agrobacteria. However, in contrast to predictions based on the targeting signal in VirB7, they distributed equally between inner and outer membrane, in accord with earlier results (14, 49).

DISCUSSION

VirB7-VirB9 form a complex in the membranes of *A. tumefaciens*. VirB7 and VirB9 are two essential components of the putative VirB transmembrane complex necessary for T-complex transfer from *A. tumefaciens* to plant cells. Deletion of either gene led to reductions in steady-state levels of several other VirB proteins, suggesting a role in assembly and/or stabilization of the transmembrane structure (6). To gain insight into their function, we performed a biochemical analysis showing that VirB7 and VirB9 interact by a covalent disulfide bond. Evidence for this derives from effects of reducing agents on their electrophoretic mobilities. While under reducing conditions, proteins of the expected molecular masses were detected, antisera to both VirB7 and VirB9 detected a 36-kDa complex under nonreducing conditions, corresponding to the sum of the combined molecular masses of VirB7 (4.5 kDa) and VirB9 (31 kDa). Further support for a VirB9-VirB7 complex derives from immunoprecipitation of the 36-kDa complex from crude lysates with VirB9-specific antibodies and release of VirB9 and VirB7 following incubation with DTT. Our results confirms earlier work which also unambiguously identified the cysteine residues involved in complex formation (1, 14, 15, 47, 49).

An assembly pathway for VirB7 and VirB9 complexes. To gain insight into the pathway leading to assembly of the VirB7-VirB9 complex, we monitored Vir protein synthesis and found that free VirB9 protein was never detected by nonreducing electrophoresis during 18 h of *vir* induction. However, a VirB9- and VirB7-cross-reacting 36-kDa product appeared as early as 2 h after *vir* induction, showing that newly synthesized VirB9 undergoes rapid complex formation with VirB7. Both antisera detected small amounts of an additional product of 30 kDa under nonreducing conditions after further induction (from 6 h on), which may result from limited degradation of VirB9. After reducing electrophoresis, a smaller, 25-kDa VirB9-cross-reacting species was also observed. The occurrence of small amounts of degradation products may reflect sensitivity of VirB9 to periplasmic proteases even after complex formation with VirB7, which is required for its stabilization (1, 15). In addition to the 36-kDa heterodimer, analysis with VirB7-specific antiserum revealed approximately equal amounts of a complex of 9 kDa, presumably a dimer of VirB7, and also lower amounts of monomeric VirB7. The apparent excess of VirB7 over VirB9 molecules may permit rapid complex formation with newly formed VirB9. Spudich et al. (47) showed that assembly of VirB7-VirB7 dimers occurs in the absence of other VirB proteins, and since stabilization of VirB9 required VirB7, they proposed that complex formation with VirB9 may result from the pool of VirB7-VirB7 dimers (15, 47). In contrast, we reproducibly detect a significant amount of monomeric VirB7 in *vir*-induced cells and propose an alternative assembly pathway to accommodate this result (Fig. 6). Molecules from the pool of free VirB7, possibly stabilized by a chaperone or Dsb (disulfide bond formation)-like enzyme (2), may undergo complex formation with newly synthesized VirB9. However, the VirB7-VirB7 dimer may assemble by an independent pathway, and since it does not stabilize the VirB complex (15), it may contribute to T-complex transfer in a different way, such as formation of a pore in the outer membrane suggested earlier by its homology to colicins (46). It will be interesting to study the enzymes involved in formation of the homo- and heterodimeric complexes of VirB7 and VirB9, which may constitute a novel disulfide bond formation pathway (47).

Lipoprotein modification may tether the VirB complex to the outer membrane. The stabilizing effect of VirB9-VirB7 on other VirB proteins may result from protein-protein interactions, and Fernandez et al. (15) provided ample genetic data supporting at least seven interacting partners: VirB4, VirB5,

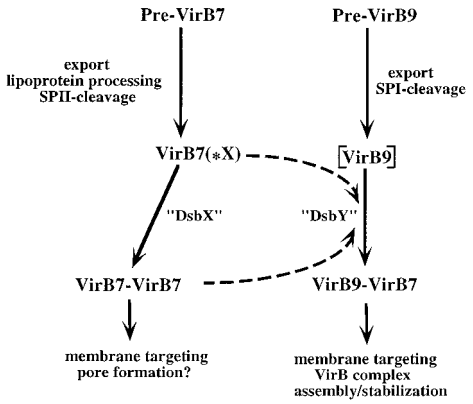

FIG. 6. Putative assembly pathway for VirB7 and VirB9 complexes. Pre-VirB7 carries an SPII cleavage site; after Sec-mediated export into the periplasm, SPII removes the signal peptide and lipoprotein processing occurs. Monomeric VirB7 may bind to a carrier protein (*X) followed by dimerization catalyzed by a Dsb-like enzyme ("DsbX") and sorting to the outer membrane. Sec-mediated export of pre-VirB9 into the periplasm and removal of the signal peptide by SPI leads to transient accumulation of VirB9 ([VirB9]). A periplasmic chaperone or Dsb-like enzyme ("DsbY") may catalyze disulfide bond formation with VirB7 from the VirB7-VirB7 dimer pool or with monomeric VirB7 (dashed arrows) followed by targeting to the outer membrane. The enzymes designated *X, "DsbX", and "DsbY" are hypothetical, and the activities may be carried out by one or more proteins. VirB7-VirB7 and VirB7-VirB9 may have different functions in T-complex transfer to plant cells. The model is based on genetic and biochemical experiments by Fernandez et al. (14, 15), Spudich et al. (47), and Anderson et al. (1) and on our results on synthesis, modification, and complex formation of VirB9 and VirB7 (this report).

and VirB7 through VirB11. Earlier studies showed that all VirB proteins localize to the membranes of *Agrobacterium* despite the fact that many, such as VirB1, VirB4, VirB5, VirB7, VirB9, and VirB11, contain few or no hydrophobic segments. These tight membrane associations may rely on protein-protein interactions with VirB2, VirB3, VirB6, VirB8, and VirB10, which contain membrane as well as periplasmic domains. Here, we showed that VirB7 and VirB9 distribute equally between the inner and outer membranes, in spite of a lipoprotein targeting signal predicting outer membrane localization of VirB7, confirming similar results by Fernandez et al. (14). VirB7 and VirB9 are likely integral parts of a transmembrane structure, and two factors may contribute to their apparent localization in the membranes. First, they may interact with other VirB proteins in either membrane, and second, lipoprotein processing may mediate outer membrane attachment of VirB7 by hydrophobic fatty acid modifications at the N terminus. However, separation of the transmembrane VirB structure imposed by shearing forces during sucrose gradient centrifugation may lead to artificial membrane localization of VirB proteins, which do not necessarily reflect the intact complex (14, 49).

VirB7 carries an SPII cleavage signal sequence; Fernandez et al. (14) demonstrated labeling with [^{3}H]palmitic acid in *E. coli*, and by Western blotting they showed inhibition of processing in *Agrobacterium* by globomycin. However, the heterologous host did not support complex formation with VirB9 (47). Here, two-dimensional electrophoretic analysis of lysates from *A. tumefaciens* grown in the presence of [^{3}H]palmitic acid demonstrated labeling of VirB7 in its 36-kDa complex with VirB9 and of the 9-kDa homodimer. The monomeric form of VirB7 could not be visualized due to interference of radiolabeled products of similar molecular mass. In addition, we isolated the ^{3}H-labeled 36-kDa complex by immunoprecipitation with VirB9-specific antiserum. Thus, we showed clearly that VirB7 undergoes lipoprotein processing in *A. tumefaciens* followed by formation of homo- and heterodimeric complexes. Additional assays, such as analysis of PhoA fusions (4, 14, 47), susceptibility to proteases (14), and cross-linking with water-soluble agents (3a), demonstrated periplasmic localization of both proteins.

Use of the yeast two-hybrid system to study protein-protein interactions in *A. tumefaciens*. Genetic and biochemical studies are beginning to unravel the protein-protein interactions involved in stabilization of the putative VirB-coded transmembrane channel, and although important progress has been made, each method has its intrinsic limits. The yeast two-hybrid system offers an independent approach to study components of T-complex transfer. To test the potential of the yeast two-hybrid system for assay of *Agrobacterium*-specific protein-protein interactions, we chose the cooperative ssDNA binding protein VirE2 (10, 11, 57). In-frame fusions of VirE2 to DBD and AD of GAL4 activated transcription of the *lacZ* gene. Thus, VirE2 binds to itself, but this affinity may be modulated by ssDNA in *Agrobacterium.*

Next, the interaction of VirB9 and VirB7 was tested. Coexpression of DBD fusion of VirB9 and AD fusion of VirB7 in Y153 led to strong transcriptional activation of the *lacZ* promoter. Quantitative experiments on the tumor suppressor protein Rb and interacting proteins suggest that this level of transcriptional activation may correspond to affinities in the nanomolar K_d range (13). This result is surprising at first, because disulfide bond formation is unlikely to occur in the reducing environment of the yeast nucleus (2). Also, the disulfide bond between cysteines 24 of VirB7 and 262 of VirB9 was shown to be crucial for their interaction and stability (1, 47), and an *Agrobacterium*-specific pathway is required for complex formation (47). Such disulfide bond formation may depend on periplasmic chaperones or disulfide bond-forming enzymes, which recognize the proteins via cysteine residues. Unproductive interaction of cysteine replacement mutants of VirB7 and VirB9 with these factors may subject them to degradation by periplasmic proteases in a similar way as misfolded subunits of P pili (22). However, the present results with the yeast two-hybrid system suggest that the affinity between VirB7 and VirB9 extends beyond their cysteine residues. Comparison with homologous proteins from the IncN conjugation system, which do not contain cysteine residues, suggests that strong protein-protein interactions may substitute for covalent bond formation (36).

Many examples validate the use of the yeast two-hybrid system for analysis of protein-protein interactions, mostly in eucaryotic (8) but also in bacterial (24, 32) systems. Here, we have shown its use for confirmation of interactions detected by other methods. However, it may be well suited for future studies on interactions between hydrophilic VirB proteins, such as VirB1, VirB4, VirB5, and VirB11. Also, our knowledge on the topology of membrane-associated VirB proteins, such as VirB8 and VirB10, may allow the construction of fusions to analyze interactions with their periplasmic domains. This strategy may greatly accelerate detailed mapping as well as mutational analysis of interacting domains (31).

ACKNOWLEDGMENTS

We thank Yuval Cohen for discussions and technical suggestions, Tim Durfee for help with the yeast two-hybrid system, and other members of the Zambryski lab for encouragement.

This work was supported by NSF grant IBN-9507782 to P.C.Z. C.B. was supported by a fellowship from the Deutsche Forschungsgemeinschaft (DFG, Ba 1416/1-1).

REFERENCES

1. **Anderson, L. B., A. Vogel Hertzel, and A. Das.** 1996. *Agrobacterium tumefaciens* VirB7 and VirB9 form a disulfide-linked protein complex. Proc. Natl. Acad. Sci. USA **93:**8889–8894.
2. **Bardwell, J. C. A., and J. Beckwith.** 1993. The bonds that tie: catalyzed disulfide bond formation. Cell **74:**769–771.
3. **Baron, C., M. Llosa, S. Zhou, and P. C. Zambryski.** 1997. VirB, a component of the T-complex transfer machinery of *Agrobacterium tumefaciens*, is processed to a C-terminal secreted product, VirB1*. J. Bacteriol. **179:**1203–1210.

3a. **Baron, C., and P. Zambryski.** Unpublished data.

4. **Beijersbergen, A., S. J. Smith, and P. J. J. Hooykaas.** 1994. Localization and topology of VirB proteins of *Agrobacterium tumefaciens*. Plasmid **32:**212–218.
5. **Berger, B. R., and P. J. Christie.** 1993. The *Agrobacterium tumefaciens virB4* gene product is an essential virulence protein requiring an intact nucleoside triphosphate-binding domain. J. Bacteriol. **175:**1723–1734.
6. **Berger, B. R., and P. J. Christie.** 1994. Genetic complementation analysis of the *Agrobacterium tumefaciens virB* operon: *virB2* through *virB11* are essential virulence genes. J. Bacteriol. **176:**3646–3660.
7. **Binns, A. N., C. E. Beaupré, and E. M. Dale.** 1995. Inhibition of VirB-mediated transfer of diverse substrates from *Agrobacterium tumefaciens* by the IncQ plasmid RSF1010. J. Bacteriol. **177:**4890–4899.
8. **Chien, C. T., P. L. Bartel, R. Sternglanz, and S. Fields.** 1991. The two-hybrid system: a method to identify and clone genes for proteins that interact with a protein of interest. Proc. Natl. Acad. Sci. USA **88:**9578–9582.
9. **Christie, P. J., J. E. Ward, M. P. Gordon, and E. W. Nester.** 1989. A gene required for transfer of T-DNA to plants encodes an ATPase with autophosphorylating activity. Proc. Natl. Acad. Sci. USA **86:**9677–9681.
10. **Christie, P. J., J. E. Ward, S. C. Winans, and E. W. Nester.** 1988. The *Agrobacterium tumefaciens virE2* gene product is a single-stranded DNA binding protein that associates with T-DNA. J. Bacteriol. **170:**2659–2667.
11. **Citovsky, V., M. L. Wong, and P. C. Zambryski.** 1989. Cooperative interaction of *Agrobacterium* VirE2 protein with single-stranded DNA: implications for the T-DNA transfer process. Proc. Natl. Acad. Sci. USA **86:**1193–1197.
12. **Durfee, T., K. Becherer, P.-L. Chen, S.-H. Yeh, Y. Yang, A. E. Kilburn, W.-H. Lee, and S. J. Elledge.** 1993. The retinoblastoma protein associates with the protein phosphatase type 1 catalytic subunit. Genes Dev. **7:**555–569.
13. **Durfee, T., B. Gorovits, C. Hensey, and W.-H. Lee.** 1996. Unpublished data.
14. **Fernandez, D., T. A. T. Dang, G. M. Spudich, X.-R. Zhou, B. R. Berger, and P. J. Christie.** 1996. The *Agrobacterium tumefaciens virB7* gene product, a proposed component of the T-complex transport apparatus, is a membrane-associated lipoprotein exposed at the periplasmic surface. J. Bacteriol. **178:** 3156–3167.
15. **Fernandez, D., G. M. Spudich, X.-R. Zhou, and P. J. Christie.** 1996. The *Agrobacterium tumefaciens virB7* lipoprotein is required for stabilization of virB proteins during assembly of the T-complex transport apparatus. J. Bacteriol. **178:**3168–3176.
16. **Finberg, K. E., T. R. Muth, S. P. Young, J. B. Maken, S. M. Heitritter, A. N. Binns, and L. M. Banta.** 1995. Interactions of VirB9, -10, and -11 with the membrane fraction of *Agrobacterium tumefaciens*: solubility studies provide evidence for tight associations. J. Bacteriol. **177:**4881–4889.
17. **Fullner, K., K. M. Stephens, and E. W. Nester.** 1994. An essential virulence protein of *Agrobacterium tumefaciens*, VirB4, requires an intact mononucleotide binding domain to function in transfer of T-DNA. Mol. Gen. Genet. **245:**704–715.
18. **Gennity, J. M., H. Kim, and M. Inouye.** 1991. The protein sequence responsible for lipoprotein localization in *Escherichia coli* exhibits remarkable specificity. J. Biol. Chem. **266:**16458–16464.
19. **Harlow, E., and D. Lane.** 1988. Antibodies: a laboratory manual. Cold Spring Harbor Laboratory, Cold Spring Harbor, N.Y.
20. **Hayashi, S., and H. C. Wu.** 1990. Lipoproteins in bacteria. J. Bioenerg. Biomembr. **22:**451–471.
21. **Hooykaas, P. J. J., and A. G. M. Beiersbergen.** 1994. The virulence system of *Agrobacterium tumefaciens*. Annu. Rev. Phytopathol. **32:**157–179.
22. **Hultgren, S. J., S. Abraham, M. Caparon, P. Falk, J. W. St. Geme III, and S. Normark.** 1993. Pilus and nonpilus bacterial adhesins: assembly and function in cell recognition. Cell **73:**887–901.
23. **Jasper, F., C. Koncz, J. Schell, and H. H. Steinbiss.** 1994. *Agrobacterium* T-strand production *in vitro*—sequence-specific cleavage and 5′-protection of single-stranded DNA templates by purified VirD2. Proc. Natl. Acad. Sci. USA **91:**694–698.
24. **Jonczyk, P., and A. Nowicka.** 1996. Specific in vivo protein-protein interactions between *Escherichia coli* SOS mutagenesis proteins. J. Bacteriol. **178:** 2580–2585.
25. **Jones, A. L., K. Shirasu, and C. I. Kado.** 1994. The product of the *virB4* gene of *Agrobacterium tumefaciens* promotes accumulation of VirB3 protein. J. Bacteriol. **176:**5255–5261.
26. **Kado, C. I.** 1994. Promiscuous DNA transfer system of *Agrobacterium tumefaciens*: role of the *virB* operon in sex pilus assembly an synthesis. Mol. Microbiol. **12:**17–22.
27. **Kuldau, G. A., G. de Vos, J. Owen, G. McCaffrey, and P. C. Zambryski.** 1990. The *virB* operon of *Agrobacterium tumefaciens* pTiC58 encodes 11 open reading frames. Mol. Gen. Genet. **221:**256–266.
28. **Laemmli, U. K.** 1970. Cleavage of structural proteins during the assembly of the head of bacteriophage T4. Nature **227:**680–685.
29. **LaVallie, E. R., E. A. DiBlasio, S. Kovacic, K. L. Grant, P. F. Schendel, and J. M. McCoy.** 1993. A thioredoxin gene fusion system that circumvents inclusion body formation in the *E. coli* cytoplasm. Bio/Technology **11:**187–193.
30. **Lessl, M., and E. Lanka.** 1994. Common mechanisms in bacterial conjugation and Ti-mediated T-DNA transfer to plant cells. Cell **77:**321–324.
31. **Marykwas, D. L., and H. C. Berg.** 1996. A mutational analysis of the interaction between FliG and FliM, two components of the flagellar motor of *Escherichia coli*. J. Bacteriol. **178:**1289–1294.
32. **Marykwas, D. L., S. A. Schmidt, and H. C. Berg.** 1996. Interacting components of the flagellar motor of *Escherichia coli* revealed by the two-hybrid system in yeast. J. Mol. Biol. **256:**564–576.
33. **Okamoto, S., A. Toyoda-Yamamoto, K. Ito, I. Takebe, and Y. Machida.** 1988. Localization and orientation of the VirD4 protein of *Agrobacterium tumefaciens* in the cell membrane. Mol. Gen. Genet. **228:**24–32.
34. **Otten, L., H. De Greve, J. Leemans, R. Hain, P. Hooykaas, and J. Schell.** 1984. Restoration of virulence of *vir* region mutants of *Agrobacterium tumefaciens* strain B6S3 by coinfection with normal and mutant *Agrobacterium* strains. Mol. Gen. Genet. **195:**159–163.
35. **Pansegrau, W., F. Schoumacher, B. Hohn, and E. Lanka.** 1993. Site-specific cleavage and joining of single-stranded DNA by VirD2 protein of *Agrobacterium tumefaciens* Ti plasmids: analogy to bacterial conjugation. Proc. Natl. Acad. Sci. USA **90:**11538–11542.
36. **Pohlman, R. F., H. D. Genetti, and S. C. Winans.** 1994. Common ancestry between IncN conjugal transfer genes and macromolecular export systems of plant and animal pathogens. Mol. Microbiol. **14:**655–668.
37. **Poquet, I., M. G. Kornacker, and A. P. Pugsley.** 1993. The role of the lipoprotein sorting signal (aspartate +2) in pullulanase secretion. Mol. Microbiol. **9:**1061–1069.
38. **Regensburg-Tuïnk, A. J. K., and P. J. J. Hooykaas.** 1993. Transgenic *N. glauca* plants expressing bacterial virulence gene *virF* are converted into hosts for nopaline strains of *A. tumefaciens*. Nature **363:**69–71.
39. **Salmond, G. P. C.** 1994. Secretion of extracellular virulence factors by plant pathogenic bacteria. Annu. Rev. Phytopathol. **32:**181–200.
40. **Salmond, G. P. C., and P. J. Reeves.** 1993. Membrane traffic wardens and protein secretion in gram-negative bacteria. Trends Biochem. Sci. **18:**7–12.
41. **Sambrook, J., E. F. Fritsch, and T. Maniatis.** 1989. Molecular cloning: a laboratory manual, 2nd ed. Cold Spring Harbor Laboratory, Cold Spring Harbor, N.Y.
42. **Schägger, H., and G. von Jagow.** 1987. Tricine-sodium dodecyl sulfate-polyacrylamide gel electrophoresis for the separation of proteins in the range of 1 to 100 kDa. Anal. Biochem. **166:**368–379.
43. **Scheiffele, P., W. Pansegrau, and E. Lanka.** 1995. Initiation of *Agrobacterium tumefaciens* T-DNA processing: purified proteins VirD1 and VirD2 catalyze site- and strand-specific cleavage of superhelical T-border DNA *in vitro*. J. Biol. Chem. **270:**1269–1276.
44. **Shirasu, K., and C. I. Kado.** 1993. Membrane localization of the Ti plasmid VirB proteins involved in the biosynthesis of a pilin-like structure in *Agrobacterium tumefaciens*. FEMS Microbiol. Lett. **111:**287–294.
45. **Shirasu, K., Z. Koukolikova-Nicola, B. Hohn, and C. I. Kado.** 1994. An inner membrane-associated virulence protein essential for T-DNA transfer from *Agrobacterium tumefaciens* to plants exhibits ATPase activity and similarities to conjugative transfer genes. Mol. Microbiol. **11:**581–588.
46. **Shirasu, K., P. Morel, and C. I. Kado.** 1990. Characterization of the *virB* operon of an *Agrobacterium tumefaciens* Ti plasmid: nucleotide sequence and protein analysis. Mol. Microbiol. **4:**1153–1163.
47. **Spudich, G. M., D. Fernandez, X.-R. Zhou, and P. J. Christie.** 1996. Intermolecular disulfide bonds stabilize VirB7 homodimers and VirB7/VirB9 heterodimers during biogenesis of the *Agrobacterium tumefaciens* T-complex transport apparatus. Proc. Natl. Acad. Sci. USA **93:**7512–7515.
48. **Sundberg, C., L. Meek, K. Carrol, A. Das, and W. Ream.** 1996. VirE1 protein mediates export of the single-stranded DNA-binding protein VirE2 from *Agrobacterium tumefaciens* into plant cells. J. Bacteriol. **178:**1207–1212.
49. **Thorstenson, Y. R., G. A. Kuldau, and P. C. Zambryski.** 1993. Subcellular localization of seven VirB proteins of *Agrobacterium tumefaciens*: implications for the formation of a T-DNA transport structure. J. Bacteriol. **175:** 5233–5241.
50. **Thorstenson, Y. R., and P. C. Zambryski.** 1994. The essential virulence protein VirB8 localizes to the inner membrane of *Agrobacterium tumefaciens*. J. Bacteriol. **176:**1711–1717.
51. **Ward, J. E., D. E. Akiyoshi, D. Regier, A. Datta, M. P. Gordon, and E. W. Nester.** 1988. Characterization of the *virB* operon from an *Agrobacterium tumefaciens* Ti plasmid. J. Biol. Chem. **263:**5804–5814.
52. **Ward, J. E., D. E. Akiyoshi, D. Regier, A. Datta, M. P. Gordon, and E. W. Nester.** 1990. Characterization of the *virB* operon from an *Agrobacterium tumefaciens* Ti plasmid. J. Biol. Chem. **265:**4768.
53. **Winans, S. C., D. L. Burns, and P. J. Christie.** 1996. Adaption of a conjugal system for the export of pathogenic macromolecules. Trends Microbiol. **4:**64–68.
54. **Yanisch-Perron, C., J. Vieira, and J. Messing.** 1985. Improved M13 phage

cloning vectors and host strains: nucleotide sequence of the M13mp18 and pUC18 vectors. Gene **33:**103–119.
55. **Zambryski, P. C.** 1992. Chronicles from the *Agrobacterium*-plant cell DNA transfer story. Annu. Rev. Plant Physiol. Plant Mol. Biol. **43:**465–490.
56. **Zambryski, P. C., H. Joos, C. Genetello, J. Leemans, M. van Montagu, and J. Schell.** 1983. Ti plasmid vector for the introduction of DNA into plant cells without alteration of their normal regeneration capacity. EMBO J. **2:**2143–2150.
57. **Zupan, J. R., V. C. Citovsky, and P. C. Zambryski.** 1996. *Agrobacterium* VirE2 protein mediates nuclear uptake of single-stranded DNA in plant cells. Proc. Natl. Acad. Sci. USA **93:**2392–2397.
58. **Zupan, J. R., and P. C. Zambryski.** The *Agrobacterium* DNA transfer complex. Submitted for publication.
59. **Zupan, J. R., and P. C. Zambryski.** 1995. Transfer of T-DNA from *Agrobacterium* to the plant cell. Plant Physiol. **107:**1041–1047.